International Journal of Engineering Science and Applied Mathematics
Volume.15, Number 5; May-2024;
ISSN: 2836-9521| Impact Factor: 6.64
https://zapjournals.com/Journals/index.php/ijesam
Published By: Zendo Academic Publishing

DYNAMIC STABILITY ASSESSMENT AND ENHANCEMENT IN THE NIGERIAN 330 KV, 36-BUS ELECTRICITY GRID NETWORK VIA COMBINED USE OF GOVERNOR AND POWER SYSTEM STABILIZER

[1]Rufus Akinnusimi Jokojeje, [1]Isaiah Adediji Adejumobi +234 906 603 2331, [1]Oluwaseun Ibrahim Adebisi +234 803 476 6428, and [2]Idowu Ademola Osinuga +234 805 623 3056
***Corresponding Author's Email: akinnusimialaba@yahoo.com/ +234 703 4630607**

Article Info
Keywords: Small signal or dynamic instability Eigenvalues, Governor, Power System Stabilizer, Rotor Angle.
DOI
10.5281/zenodo.11198217

Abstract
Small signal or dynamic instability is one of the major challenges experienced in the operation of power systems, which often results in the violation of acceptable voltage and frequency limits. Therefore, this study assessed small signal stability on a power system via an eigenvalues approach. Non-linear differential-algebraic equations describing the dynamic characteristics of the power system were developed. These equations were linearized using Taylor's series expansion. The computational algorithm with eigenvalues was developed considering the Nigerian 330 kV electricity grid comprising 13 generators and 36 busses as test system. The qualitative stability state of the system was determined by obtaining the eigenvalues of the generator rotor angle (δ) parameters with and without control schemes implemented via the governor (G) and the governor with the power system stabilizer (G + PSS). The results showed that δ was in stable state for all 13 generators in the network with eigenvalues obtained having negative real parts with and without controllers; although a better system stability level was obtained with G + PSS compared to G because the real part of the obtained eigenvalues was much lower in value. This result clearly revealed that G + PSS exhibited superiority over G in improving the small signal stability of the considered power network. The use of eigenvalues produced a simplified analysis of the small signal stability of a power system network where the combined effect of the governor and power system stabilizer offered better stability enhancement.

[1] Department of Electrical and Electronics Engineering, College of Engineering, Federal University of Agriculture, Abeokuta, Nigeria
[2] Department of Mathematics, College of Physical Sciences, Federal University of Agriculture, Abeokuta, Nigeria

1. INTRODUCTION

One of the key elements responsible for the continuous running of an interconnected power system is the system generators. Generators, during normal operation, may encounter disturbances like sustained oscillations in speed or periodic torque variations. These disruptions can lead to voltage or frequency fluctuations, negatively impacting the operation of other interconnected power system components, which in most cases results in loss of synchronism (Afzal *et al*., 2021; Mohammed et al., 2015). Alongside these disturbances, other critical issues such as steady-state stability, transient stability, dynamic stability, harmonics, disturbances, voltage collapse, and reactive power loss require careful attention in power system management to ensure optimal performance. Neglecting these concerns may lead to persistent instability in system operations (Afzal *et al*., 2021; Mohammed et al., 2015).

This work focuses on the assessment of dynamic stability because of its inherent importance for optimizing the performance of an interconnected power system. Dynamic stability is associated with a system operating normally without any major disturbance. It describes the characteristics of the system when subjected to small disturbances such as small changes in load, voltage, frequency, and rotor angle. Present-day interconnected power systems are typical examples of large-scale complex multivariate systems. They generally comprise several dynamic units, including synchronous generators and dynamic loads, such as synchronous and induction motors. The generated electrical energy is transmitted over an interconnecting network, which in turn supplies the required power to load centres. Much of the complexity in these systems arises from the fact that in the analysis of any one segment of the system, the whole interconnected system needs to be considered (Gomila *et al*., 2023; El Din, 1977), and the problems involved are always associated with the inclusion of damping of mechanical oscillations and the stability of the frequency control loop.

The power system dynamic stability characteristics are of great significance to power system engineers and researchers. Dynamic stability characteristics of systems have been recognized as essential for secure and quality system operation (Yousif *et al.*, 2022; Bayliss and Hardy, 2007). The problems and effects involved in power system dynamic studies have always been associated with the question of whether or not a system remains in synchronism after a credible disturbance (Shrestha *et al.*, 2021; deMello, 1975). Dynamic problems in power systems have been classified under the major categories of electrical machine and system dynamics, system governing and generation controls, and prime-mover energy supply system dynamics and controls (Kawther *et al.*, 2021; deMello, 1975). Usually, the second class of dynamics lasts for many minutes, whereas the third class of dynamics lasts for several seconds to a few minutes. Hence, for the analysis of system dynamics included in these two classes, the network and machine electrical transients can be neglected. The first class of dynamics is the most involved in stability studies performed by electrical utilities. It is related to machine and system dynamics; hence, the interaction between machines, excitation systems, turbine governors, and system loads should be considered. Usually, the simulated dynamics in this class result in relatively large equivalent systems. These, in turn, require efficient modeling and analysis techniques. Concurrent with these requirements is the need for a good understanding of the fundamentals and physics involved in system interactions. Hence, this work dealt with significance of this work: dynamic stability assessment and enhancement in the Nigerian 330 kV, 36-bus electricity grid network via the combined use of governor and power system stabilizer.

2 Methodology

The Nigerian 330 KV, 36-bus system was modeled as a case study of the power system for the simulation experiment. MATLAB codes were developed for modeling the interconnected power system with damping controllers and for programing the eigenvalue stability analyzer. Simulations were carried out to determine the effect on the rotor angle stability of the case study of the power system. The stability of the 36-bus case study interconnected power network is evaluated with a power system network with a governor and a governor + power system stabilizer (G +PSS) as damping controllers.

3 Mathematical Model of Vector Matrixes for Eigenvalue Analysis

Power system matrices are required for the stability analyses of the eigenvalue program; hence, the mathematical model was derived as shown:

4 Classical Model of Synchronous Machines (Generator)

Generator Represented by the Classical Model

With the generator represented by the classic model and all resistances neglected, the system representation is shown in Figure 5.

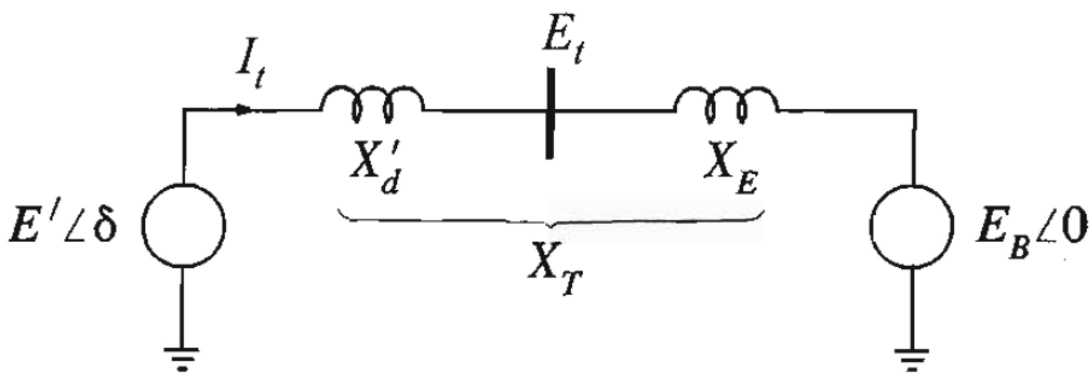

Figure 1: Classical Model of a Generator for an Infinite Bus (Kundur 2004)

Here E' is the voltage behind X'_d. Its magnitude is assumed to remain constant at the predisturbance value. Let δ be the angle by which E' leads the infinite bus voltage E_B. As the rotor oscillates during a disturbance, δ changes. With E' as reference phasor,

$$\tilde{I}_t = \frac{E'\angle 0^0 - E_B\angle -\delta}{jX_T} = \frac{E' - E_B(\cos\delta - j\sin\delta)\angle -\delta}{jX_T} \qquad \text{Equation (1)}$$

The complex power behind X'_d is given by

$$S' = P + jQ' = \tilde{E}'\tilde{I}_t^* = \frac{E'E_B\sin\delta}{jX_T} + j\frac{E\prime(E' - E_B\cos\delta)}{X_T} \qquad \text{Equation (2)}$$

With the stator resistance neglected, the air-gap power P_e is equal to the terminal power P. In per unit, the air-gap torque is equal to the air-gap power.

$$T_e = P = \frac{E'E_B}{X_T}\sin\delta \qquad \text{Equation (3)}$$

Linearizing the initial operating condition represented by $\delta = \delta_0$ yields

$$\Delta T_e = \frac{\partial T_e}{\partial\delta}\Delta\delta = \frac{E'E_B}{X_T}\mathrm{Cos}\,\delta_0\,\Delta\delta \qquad \text{Equation (4)}$$

The equations of motion per unit are

$$p\Delta\omega_r = \frac{1}{2H}(T_m - T_e - K_D\Delta\omega_r) \qquad \text{Equation (5)}$$

$$p\delta = \omega_0\Delta\omega_r \qquad \text{Equation (6)}$$

Where $\Delta\omega_r$ is the per unit speed deviation, δ is the rotor angle in electrical radians, ω_0 is the base rotor electrical speed in radians per second and p is the differential operator d/dt with time t in seconds.

Linearizing Equation (5) and substituting for ΔT_e given by Equation (4), we obtain

$$p\Delta\omega_r = \frac{1}{2H}(\Delta T_m - K_s\Delta\delta - K_D\Delta\omega_r) \qquad \text{or}$$

$$p\Delta f_r = 2\pi^{-1}\left[\frac{1}{2H}(\Delta T_m - K_s\Delta\delta - K_D\Delta\omega_r)\right] \qquad \text{Equation (7)}$$

Where K_s is the synchronizing torque coefficient given by

$$K_s = \left(\frac{E'E_B}{X_T}\right)\mathrm{Cos}\,\delta_0 \qquad \text{Equation (8)}$$

Linearizing Equation (6), we obtain

$$p\Delta\delta = \omega_0\Delta\omega_r \qquad \text{Equation (9)}$$

By writing Equations (7) and (8) in vector-matrix form, we obtain

$$\frac{d}{dt}\begin{bmatrix}\Delta\omega_r\\ \Delta\delta\end{bmatrix} = \begin{bmatrix}-\frac{K_D}{2H} & -\frac{K_S}{2H}\\ \omega_0 & 0\end{bmatrix}\begin{bmatrix}\Delta\omega_r\\ \Delta\delta\end{bmatrix} + \begin{bmatrix}\frac{1}{2H}\\ 0\end{bmatrix}\Delta T_m \qquad \text{Equation (10)}$$

$$x^T = (\Delta\omega \quad \Delta\delta) \qquad \text{Equation (11)}$$

Equation (11) represents the variable of interest during machine operation.

The block diagram shown in Figure 6 can be used to describe the small-signal performance.

Where

$\Delta\omega_r =$ per unit speed deviation

$\delta =$ rotor angle in electrical radians

$\omega_0 =$ base rotor electrical speed in radians per second $= 2\pi f_o$

$f_o =$ fundamental frequency in Hz

$p =$ differential operator d/dt with time t in seconds

$H =$ Inertia constant

$T_{\mathrm{m}} =$ Mechanical torque

T_e = Electrical torque with $\Delta T_e = \frac{\partial T_e}{\partial\delta}\Delta\delta = \frac{E'E_B}{X_T}cos\delta_0(\Delta\delta) = K_s\Delta\delta)$

$K_s =$ the synchronizing torque $coefficient$ given by equation $= \left(\frac{E'E_B}{X_T}\right)cos\delta_0$

When the flux linkage effect is considered, the field circuit dynamic equation (12) is obtained:

$$p\psi_{fd} = \omega_0\left(e_{fd} - R_{fd}i_{fd}\right) = \frac{\omega_0 R_{fd}}{L_{adu}}E_{fd} - \omega_0 R_{fd}i_{fd} \qquad \text{Equation (12)}$$

Where

$E_{fd} =$ Exciter output voltage

$e_{fd} =$ Rotor field voltage

$R_{fd} =$ Rotor field resistance

$i_{fd} =$ Rotor field current

Equations (5) and (6) together with equation (12) describe the dynamics of the synchronous machine with $\Delta\omega_r$, $\Delta\delta$, and $\Delta\psi_{fd}$ (rotor flux linkage) as state variables. However, the derivatives of these state variables appear in these equations as functions of T_e and i_{fd}, which are neither state variables nor input variables. This therefore requires that i_{fd} and T_e are expressed in terms of the state variables to develop the complete system equations in the state-space form for the classical generator model. This requirement gives rise to equations (12) and (13) and their manipulation with equations (5), (6), and (13) leads to equation (14) that gives the desired final form for classical generator model dynamics.

$$\Delta i_{fd} = \frac{\psi_{fd} - \psi_{ad}}{L_{fd}} = \frac{1}{L_{fd}}\left(1 - \frac{L'_{ads}}{L_{fd}} + m_2 L'_{ads}\right)\Delta\psi_{fd} + \frac{1}{L_{fd}}m_1 L'_{ads}\Delta\delta \qquad \text{Equation (13)}$$

$$\Delta T_e = \psi_{ad0}\Delta i_q + i_{q0}\Delta\psi_{ad} - \psi_{aq0}\Delta i_d - i_{d0}\Delta\psi_{aq} = K_1\Delta\delta + K_2\Delta\psi_{fd} \qquad \text{Equation (14)}$$

Where

$$K_1 = n_1(\psi_{ad0} + L_{aqs} i_{d0}) - m_2(\psi_{aq0} + L'_{ads} i_{q0})$$

$$K_2 = n_2(\psi_{ad0} + L_{aqs} i_{d0}) - m_2(\psi_{aq0} + L'_{ads} i_{q0}) + \frac{L'_{ads}}{L_{fd}} i_{q0}$$

$$\begin{bmatrix} \Delta\dot{\omega}_r \\ \Delta\dot{\delta} \\ \Delta\dot{\psi}_{fd} \end{bmatrix} = \begin{bmatrix} a_{11} & a_{12} & a_{13} \\ a_{21} & 0 & 0 \\ 0 & a_{32} & a_{33} \end{bmatrix} \begin{bmatrix} \Delta\omega \\ \Delta\delta \\ \Delta\psi_{fd} \end{bmatrix} + \begin{bmatrix} b_{11} & 0 \\ 0 & 0 \\ 0 & b_{32} \end{bmatrix} \begin{bmatrix} \Delta T_m \\ \Delta E_{fd} \end{bmatrix} \quad \text{Equation (15)}$$

$x^T = (\Delta\omega \quad \Delta\delta \quad \Delta\psi_{fd})$ Variable of interest Equation (16)

ΔT_m and ΔE_{fd} depend on the prime-mover and excitation controls, and with constant mechanical input and constant exciter output voltage, ΔT_m and ΔE_{fd} are, respectively, zero. The mutual inductances L_{ads} and L_{aqs} are saturated values.

5 Modeling of a Synchronous Machine with associated Controllers

6 Governor

The governor or admission valves, also known as control valves (CV), are located in the turbine steam chest and control the flow of steam to the high-pressure turbine. The number of governor valves depends on the unit size. The governor valves control the quantity of steam flowing to the turbine by changing the valve position. The mechanical power developed by the HP turbine depends on the amount of steam flow admitted to the turbine through the valve.

sing perturbed values, the state equation of the exciter model

$$p\Delta v_1 = \frac{1}{T_R}(\Delta E_t - \Delta v_1) \quad \text{Equation (17)}$$

Where Δv_1 = Perturbed input voltage to the exciter.

$$p\Delta v_1 = \frac{K_5}{T_R}\Delta\delta + \frac{K_6}{T_R}\Delta\psi_{fd} - \frac{1}{T_R}\Delta v_1 \quad \text{Equation (18)}$$

The exciter field voltage is given by equation (18), while the perturbed form is given by equation (19):

$$E_{fd} = K_A(V_{ref} - v_1) \quad \text{Equation (19)}$$

Where K_A = Exciter gain

V_{ref} = Reference voltage

$$\Delta E_{fd} = K_A(-\Delta v_1) \quad \text{Equation (20)}$$

The field circuit dynamic equation developed in equation (15) with the effect of the excitation system included results in equation (21) (Kundur, 1994):

$$p\Delta\psi_{fd} = a_{31}\Delta\omega_r + a_{32}\Delta\delta + a_{33}\Delta\psi_{fd} + a_{34}\Delta v_1 \quad \text{Equation (21)}$$

The expressions a_{31}, a_{32}, and a_{33} remain unchanged and are given by equation (15). Since the exciter model is of first-order, the order of the overall system is increased by 1 and the new state variable added is Δv_1 leading to equation (22):

$$p\Delta v_1 = a_{41}\Delta\omega_r + a_{42}\Delta\delta + a_{43}\Delta\psi_{fd} + a_{44}\Delta v_1 \quad \text{Equation (22)}$$

The complete state-space model for the power system with the excitation system included is expressed by equation (24):

$$\begin{bmatrix} \Delta\dot{\omega}_r \\ \Delta\dot{\delta} \\ \Delta\dot{\psi}_{fd} \\ \Delta\dot{v}_1 \end{bmatrix} = \begin{bmatrix} a_{11} & a_{12} & a_{13} & 0 \\ a_{21} & 0 & 0 & 0 \\ 0 & a_{32} & a_{33} & a_{34} \\ 0 & a_{42} & a_{43} & a_{44} \end{bmatrix} \begin{bmatrix} \Delta\omega_r \\ \Delta\delta \\ \Delta\psi_{fd} \\ \Delta v_1 \end{bmatrix} + \begin{bmatrix} b_1 \\ 0 \\ 0 \\ 0 \end{bmatrix} \Delta T_m \qquad \text{Equation (24)}$$

With a constant mechanical torque input, $\Delta T_m = 0$.

The linearized state equation for the stabilizer is given by Eq. (25):

$$p\Delta v_2 = K_{STAB} p\Delta\omega_r - \frac{1}{T_W}\Delta v_2 \qquad \text{Equation (25)}$$

Where K_{STAB} is the stabilizer gain, Δv_2 is the perturbed input signal for compensation. Using the expression for $p\Delta\omega_r$ given by Eq. (15), an expression for $p\Delta v_2$ in terms of the state variables is obtained in Eq. (26) and modified in Eq. (27):

$$p\Delta v_2 = K_{STAB}\left[a_{11}\Delta\omega_r + a_{12}\Delta\delta + a_{13}\Delta\Psi_{fd} + \frac{1}{2H}\Delta T_m\right] - \frac{1}{T_W}\Delta v_2 \qquad \text{Equation (26)}$$

$$p\Delta v_2 = a_{51}\Delta\omega_r + a_{52}\Delta\delta + a_{53}\Delta\Psi_{fd} + a_{55}\Delta v_2 + \frac{K_{STAB}}{2H}\Delta T_m \qquad \text{Equation (27)}$$

$$p\Delta v_s = \frac{T_1}{T_2}\Delta v_s + \frac{1}{T_2}\Delta v_2 - \frac{1}{T_2}\Delta v_s \qquad \text{Equation (28)}$$

The use of equation (27) in equation (28) results in equation (29) given as follows:

$$p\Delta v_s = a_{61}\Delta\omega_r + a_{62}\Delta\delta + a_{63}\Delta\Psi_{fd} + a_{64}\Delta v_1 + a_{65}\Delta v_2 + a_{66}\Delta v_s + \frac{T_1}{T_2}\frac{K_{STAB}}{2H}\Delta T_m$$

The perturbed field voltage of the exciter is given by Eq. (29):

$$\Delta E_{fd} = K_A(\Delta v_s - \Delta v_1) \qquad \text{Equation (29)}$$

Hence, the field circuit equation with PSS included is given by equation (30), and the complete state-space model, including PSS (with $\Delta T_m = 0$) is given by equation (31).

$$p\Delta\Psi_{fd} = a_{32}\Delta\delta + a_{33}\Delta\Psi_{fd} + a_{34}\Delta v_1 + a_{36}\Delta v_s \qquad \text{Equation (30)}$$

$$\begin{bmatrix} \Delta\dot{\omega}_r \\ \Delta\dot{\delta} \\ \Delta\dot{\Psi}_{fd} \\ \Delta\dot{v}_1 \\ \Delta\dot{v}_2 \\ \Delta\dot{v}_s \end{bmatrix} = \begin{bmatrix} a_{11} & a_{12} & a_{13} & 0 & 0 & 0 \\ a_{21} & 0 & 0 & 0 & 0 & 0 \\ 0 & a_{32} & a_{33} & a_{34} & 0 & a_{36} \\ 0 & a_{42} & a_{43} & a_{44} & 0 & 0 \\ a_{51} & a_{52} & a_{53} & 0 & a_{55} & 0 \\ a_{61} & a_{62} & a_{63} & 0 & a_{65} & a_{66} \end{bmatrix} \begin{bmatrix} \Delta\omega_r \\ \Delta\delta \\ \Delta\Psi_{fd} \\ \Delta v_1 \\ \Delta v_2 \\ \Delta v_s \end{bmatrix} \qquad \text{Equation (31)}$$

The following should be noted:

The time frame of interest in transient stability studies is usually 3–5 s following the disturbance. It may extend to 10–20 s for numerous systems with dominant inter-area swings.

The time frame of interest in small-disturbance stability studies is on the order of 10–20 s following a disturbance. Dynamic stability, along with transient stability, voltage stability, and frequency stability, is the basic requirement for a power system to maintain secure operation (Kundur, 1994). However, the time frame of interest is extended to 25 s due to the small nature of its disturbance.

7 Dynamic Stability Assessment Using the Eigenvalue Method

The state equations (3.107) and (3.108) can be transformed to the frequency domain by Laplace transform as given by equations (3.126) and (3.127) (Xiaokang, 1999; Kundur, 1994):

$$\mathrm{s}\Delta\mathrm{x}(\mathrm{s}) - \Delta\mathrm{x}(0) = \mathrm{A}\Delta\mathrm{x}(\mathrm{s}) + \mathrm{B}\Delta\mathrm{u}(\mathrm{s}) \qquad \text{Equation (32)}$$

$$\mathrm{s}\Delta\mathrm{y}(\mathrm{s}) = \mathrm{C}\Delta\mathrm{x}(\mathrm{s}) + \mathrm{D}\Delta\mathrm{u}(\mathrm{s}) \qquad \text{Equation (33)}$$

A block diagram of the state-space representation is shown in Figure 11.

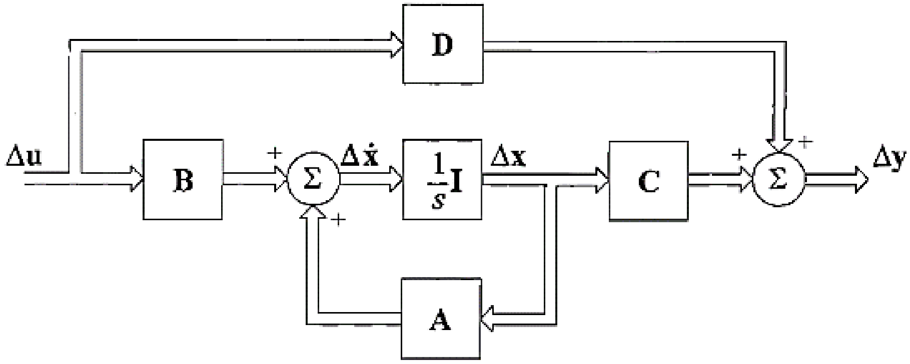

Figure 11: Block diagram of state-space representation (Xiaokang, 1999; Kundur, 1994)

A formal solution of the state equations can be obtained by equations (34) to (36) (Xiaokang, 1999; Kundur, 1994):

$$(sI - A)\Delta x(s) = \Delta x(0) + B\Delta u(s) \qquad \text{Equation (34)}$$

$$\Delta x(s) = (sI - A)^{-1}[\Delta x(0) + B\Delta u(s)] = \frac{\text{adj }(sI-A)}{\det(sI-A)}\left(\Delta x(0) + B\Delta u(s)\right) \qquad \text{Equation (35)}$$

$$\Delta y(s) = C\frac{\text{adj }(sI-A)}{\det(sI-A)}[\Delta x(0) + B\Delta u(s)] + D\Delta u(s) \qquad \text{Equation (36)}$$

Where

I = identity matrix of the same dimension as matrix A.

$\det(sI - A)$ = determinant of the matrix $(sI - A)$

adj $(sI - A)$ = adjoint of matrix $(sI - A)$

x(0) = state at time t = 0

The poles of $\Delta x(s)$ and $\Delta y(s)$ are the roots of equation (37) (Xiaokang, 1999; Kundur, 1994):

$$\det(sI - A) = 0 \qquad \text{Equation (37)}$$

Equation (37) is called the characteristic equation of matrix A (Kundur, 1994). The number of poles is equal to the number of states (Xiaokang, 1999). The values of s that satisfy equation (37) are a function of the state matrix A and are called the eigenvalues of matrix A (Xiaokang, 1999; Kundur, 1994).

For small disturbances, the linearized model of any power system can be analyzed to assess its stability using many useful tools. One such valuable tool is the eigenvalue technique. Eigenvalues provide significant information on system stability and how close the system is to becoming unstable (Kim and Overbye, 2015). It also shows the frequencies and modes that exist in the system, and how the system states interact with these modes. Hence, for a stable system, all the poles of the characteristic equation have negative real parts, i.e., all the eigenvalues lie in the left half of the complex s plane. For an unstable system, at least one pole or eigenvalue has a positive real part. Therefore, eigenvalues, also referred to as system modes, represent the dynamic performance of the system (Xiaokang, 1999; Kundur, 1994).

Referring to equation (37), for each eigenvalue λ_I (where λ has replaced s), the n-column vector ϕ_I which satisfies the equation can be obtained from equation (38) as follows:

$$A\phi_i = \lambda_i\phi_i \qquad \text{for i = 1, 2, …, n} \qquad \text{Equation (38)}$$

The column vector ϕ_I is called the right eigenvector of A associated with the eigenvalue λ_i. The dimension of ϕ_I is equal to the number of state variables and ϕ_I gives information about the mode shape (i.e., the relative activity of the state variables when a particular mode is excited) (Xiaokang, 1999; Kundur, 1994).

Similarly, there exists an n-row vector ψ_i which satisfies the equation (39) given by

$$A\psi_i = \lambda_i\psi_i \qquad for\ i = 1, 2, \ldots, n \qquad \text{Equation (39)}$$

The row vector ψ_i is called the left eigenvector of A associated with the eigenvalue λ_I and it measures the contribution of the activity of the state variables to a particular mode (Xiaokang, 1999; Kundur, 1994).

The eigenvalues of a matrix are given by the values of the scalar parameter λ for which there exist non-trivial solutions (i.e., other than $\boldsymbol{\phi} = 0$) to the equation

$$A\phi = \lambda\phi \qquad \text{Equation (40)}$$

Where

$\boldsymbol{A}$ is an n n matrix (real for a physical system such as a power system)

$\boldsymbol{\phi}$ is an $nx1$ vector

To find the eigenvalues, equation (41) can be written in the form of

$$(A - \lambda I)\phi = 0 \qquad \text{Equation (41)}$$

For a non-trivial solution

$$(\det(A - \lambda I) = 0 \qquad \text{Equation (42)}$$

The expansion of the determinate gives the characteristic equation. The $\boldsymbol{n}$ solution of $\boldsymbol{\lambda} = \boldsymbol{\lambda_1}, \boldsymbol{\lambda_2}, \ldots, \boldsymbol{\lambda_n}$ are eigenvalues of $\boldsymbol{A}$

The eigenvalues may be real or complex. If $\boldsymbol{A}$ is real, complex eigenvalues always occur in conjugate pairs.

For any eigenvalue λ_i, the $\boldsymbol{n}$-column vector ϕ_i which satisfies Equation (41) is called the right eigenvector of A associated with the eigenvalue λ_i

Because equation (42) is homogeneous, $k\phi_i$ (where k is a scalar) is also a solution. Thus, the eigenvectors are determined only within a scalar multiplier.

Is called the left eigenvector associated with the eigenvalue λ_i

The left and right eigenvectors corresponding to different eigenvalues are orthogonal. In other words, if λ_i is not equal to λ_j,

$$\psi_j\phi_i = 0 \qquad \text{Equation (43)}$$

However, for eigenvectors corresponding to the same eigenvalue,

$$\psi_i\phi_i = C_i \qquad \text{Equation (44)}$$

Where C_i is a nonzero constant.

Because, as noted above, the eigenvectors are determined only to within a scalar multiplier, it is common practice to normalize these vectors so that

$$\psi_i\phi_i = 1 \qquad \text{Equation (45)}$$

To briefly express the Eigen properties of **A**, it is convenient to introduce the following matrices:

$$\Phi = [\phi_1, \phi_2, \ldots \ldots \phi_n] \qquad \text{Equation (46)}$$

$$\Psi = [\psi_1^T \quad \psi_2^T \quad \cdots \quad \psi_n^T]^T \qquad \text{Equation (47)}$$

$\wedge$ = diagonal matrix, with the eigenvalues $\lambda_1, \lambda_2, \ldots \ldots \lambda_n$ as diagonal elements

Each of the above matrices is nxn. In terms of these matrices, equations (39) and (45) can be expanded as follows.

$$A\Phi = \Phi \wedge \qquad \text{Equation (48)}$$

$$\Psi\Phi = I\Psi = \Phi^{-1} \qquad \text{Equation (49)}$$

If follows from equation (48)

$$\Phi^{-1}A\Phi = \wedge \quad \text{Equation (50)}$$

Considering the state equation of with this equation, $\Delta y = C\Delta x + D\Delta u$,the free motion is given by

$$\Delta\dot{x} = A\,\Delta x \quad \text{Equation (51)}$$

To isolate the parameters that influence the motion in a significant way and to eliminate the cross-coupling between the state variables, a new state vector Z related to the original state vector Δx by the transformation is considered.

$$\Delta x = \Phi z \quad \text{Equation (52)}$$

Where ϕ is the modal matrix of **A** defined by equation (46) substituting Equation (52) for Δx in the state equation of (51), equation (53) is derived as follows:

$$\Phi\dot{z} = A\Phi z \quad \text{Equation (53)}$$

Hence, the new state equation can be written as

$$\dot{z} = \Phi^{-1}\boldsymbol{A}\Phi z \quad \text{Equation (54)}$$

In view of equation (50), equation (54) becomes equation (55)

$$\dot{z} = \wedge z \quad \text{Equation (55)}$$

From equation (51), A in general, is a non-diagonal matrix, whereas $\wedge$ in equation (55) is a diagonal matrix. Equation (51) represents n uncoupled first-order (scalar) equations:

$$\dot{z}_i = \lambda_i z_i \qquad i = 1,2, \dots\dots\dots. n \quad \text{Equation (56)}$$

Equation (52) was transformed to uncouple the state equations. Therefore, is to uncouple the state equations. Equation (57) is a simple first-order differential equation whose solution with respect to time t is given (57)

$$z_i(t) = z_i(0)e^{\lambda_i t} \quad \text{Equation (57)}$$

Where $z_i(0)$ is the initial value of z_i.

From Eq. (52), the response in terms of the original state vector is given by Eq. (58)

$$\Delta x(t) = \phi z(t) = [\phi_1 \quad \phi_2 \quad \cdots \quad \phi_n]\begin{bmatrix} z_1(t) \\ z_2(t) \\ \vdots \\ z_n(t) \end{bmatrix} \quad \text{Equation (58)}$$

This implies that equation (57) gives equation (59)

$$\Delta x(t) = \sum_{i=1}^{n} \phi_i\, z_i(0)e^{\lambda_i t} \quad \text{Equation (59)}$$

From equation (57), equation (60) is obtained

$$z_i(t) = \Phi^{-1}\Delta x(t) = \Psi\Delta x(t) \quad \text{Equation (60)}$$

Equation (58) can be written as equation (61):

$$z_i(t) = \psi\Delta x(t) \quad \text{Equation (61)}$$

With $\boldsymbol{t = 0}$, it follows that

$$z_i(0) = \psi_i\Delta x(0) \quad \text{Equation (62)}$$

By using c_i to denote the scalar product $\psi_i\Delta x(0)$, equation (59) may be written as follows:

$$\Delta x(t) = \sum_{i=1}^{n} \phi_i\, c_i e^{\lambda_i t} \quad \text{Equation (63)}$$

i. Real eigenvalue corresponds to the non-oscillatory mode.
ii. A negative real eigenvalue indicates a mode that decays over time
iii. (the larger the magnitude of the eigenvalue the quicker the decay).

iv. A positive real eigenvalue indicates a mode that grows with time and that the system will experience aperiodic instability.

v. Conjugate pair complex eigenvalues indicate oscillatory modes of response. $\lambda = \sigma \pm j\omega$

vi. If a conjugate of a pair of complex eigenvalues has negative real parts σ this corresponds to an oscillatory mode that decays with time, and the system is said to be globally stable.

vii. If a pair has positive real parts, the corresponding oscillatory mode grows exponentially with time and eventually dominates the system behavior. Such a system is considered unstable.

viii. If any one of the eigenvalues has a real part, the system will have an undamped oscillatory response.

8 Results and Discussion

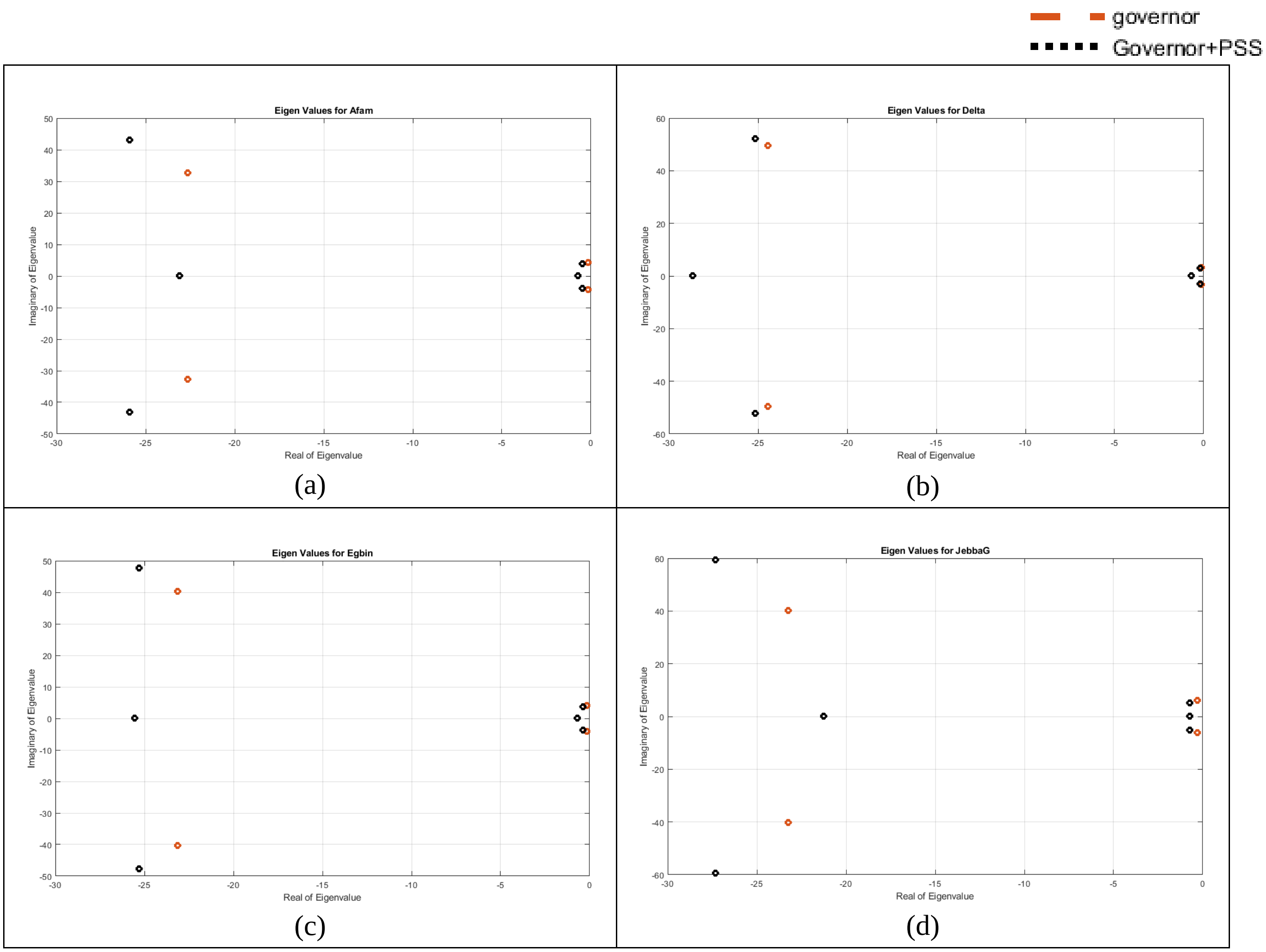

Figure 1: Signal graph of real and imaginary eigenvalues of rotor angle for
(a) Afam (b) Delta (c) Egbin and (d) Jebba-G.

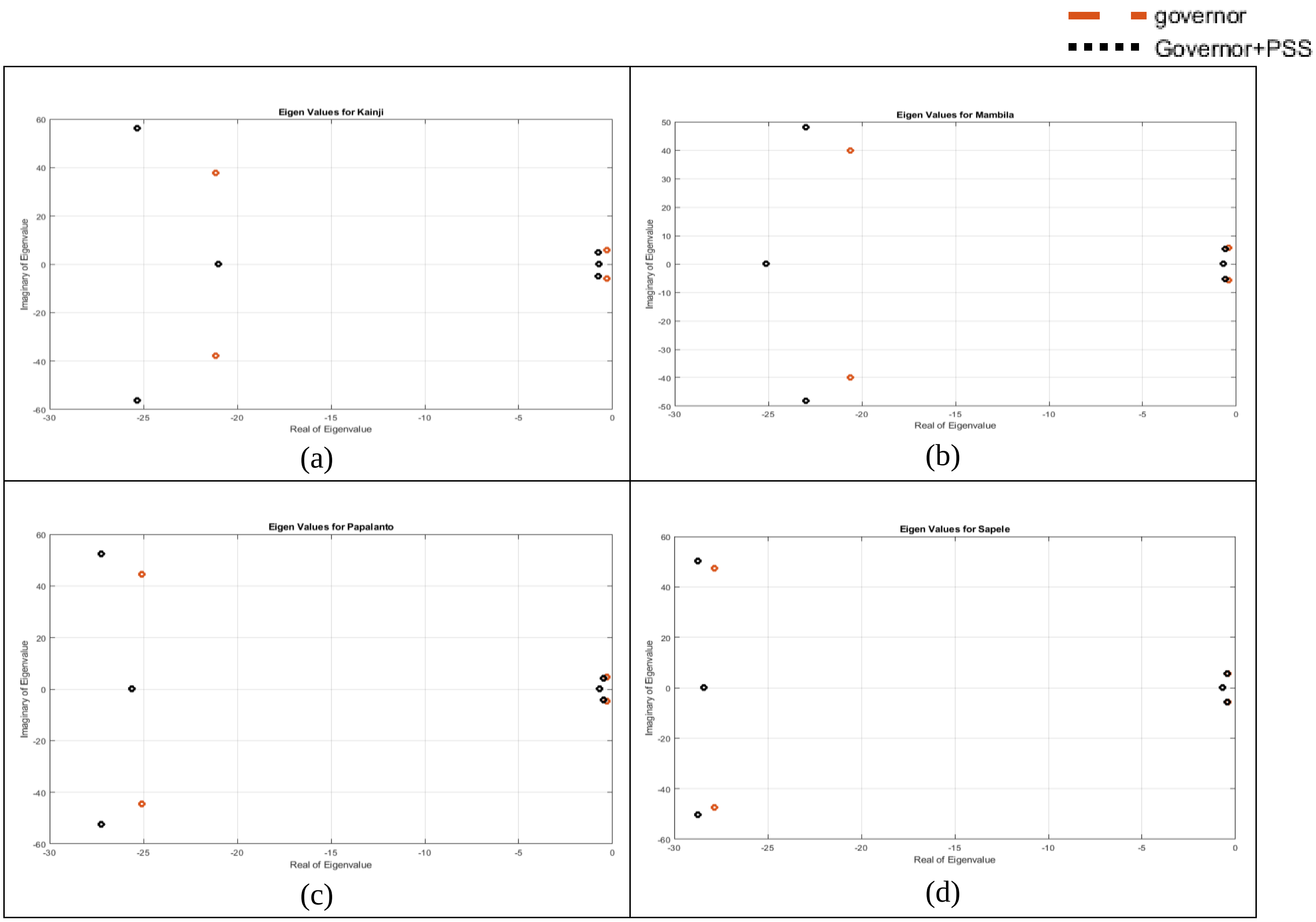

Figure 2: Signal graph of real and imaginary eigenvalues of rotor angle for (a) Kanji (b) Mambilla (c) Papalanto, and (d) Sapele.

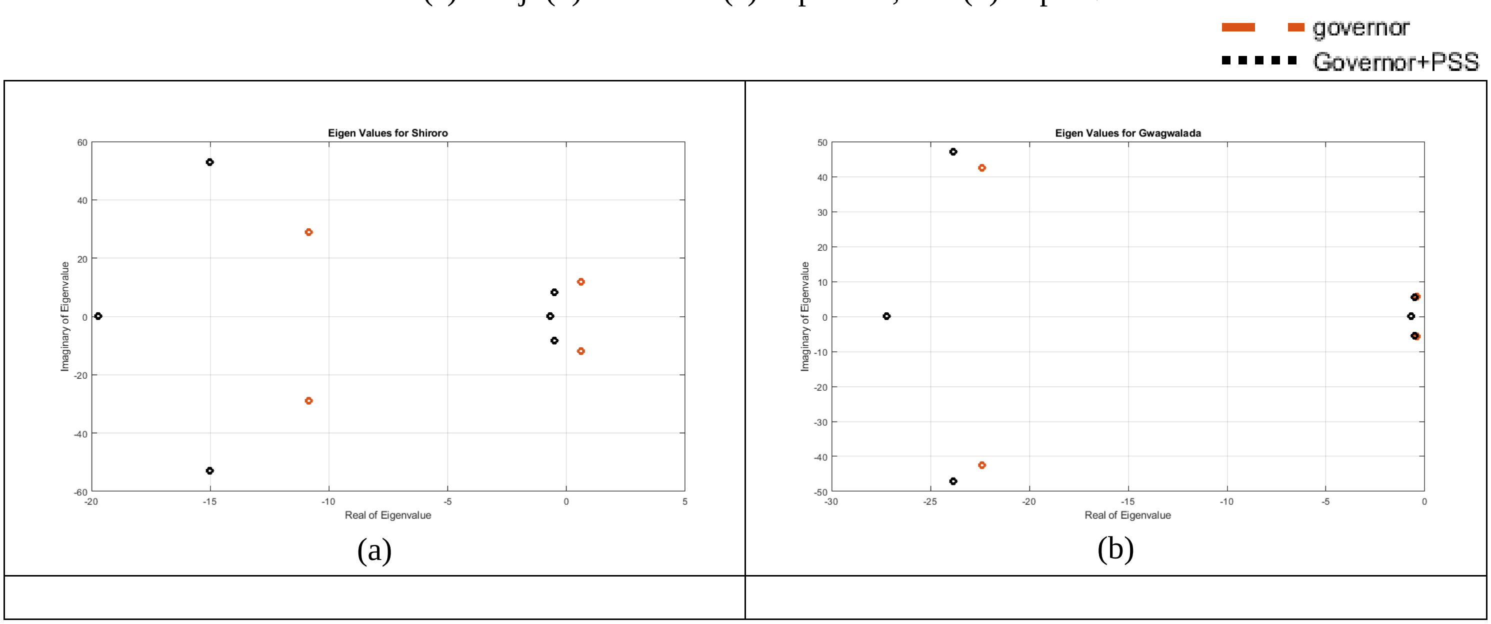

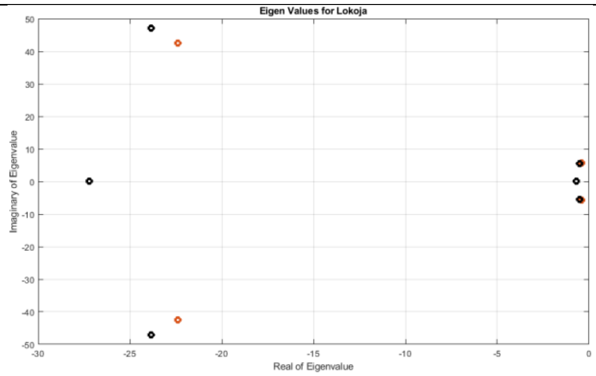

(c)

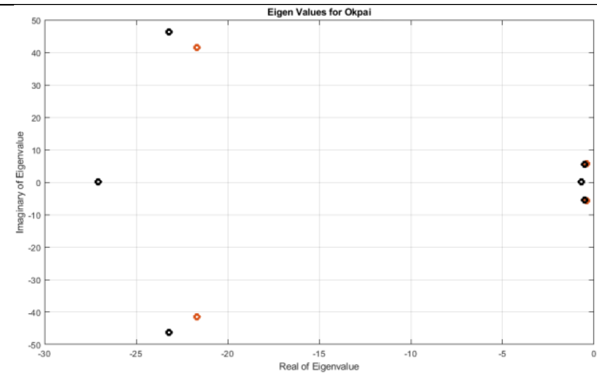

(d)

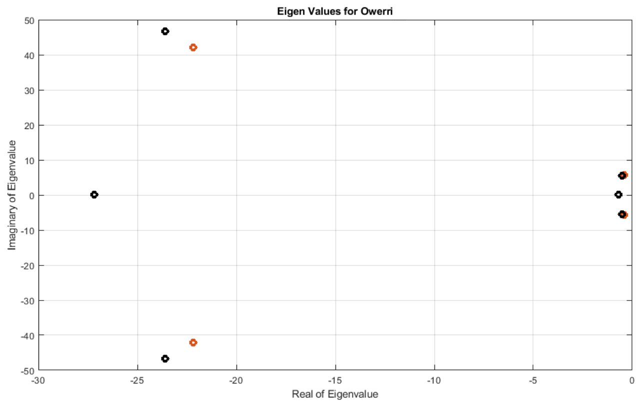

(e)

Figure 3: Signal graph of real and imaginary eigenvalues of rotor angle for
(a) Shiroro (b) Gwagwalada (c) Lokoja (d) Okpai and (e) Owerri.
(b)

Table 1: Comparative analysis of the eigenvalue results of Rotor Angle (Without Governor, With Governor and With Governor + Power System Stabilizer)

		Without Governor	With Governor	Governor + PSS
S/N	STATION	$\Delta\delta$	$\Delta\delta$	$\Delta\delta$
1	Afam	-0.14418 - j4.38057	-0.14418 - j4.38057	-25.9487 - j43.3075
2	Delta	-0.12889 - j3.14	-0.12889 - j3.14	-25.1746 - j52.2164
3	Egbin	-0.146466 - j4.08662	-0.146466 - j4.08662	-25.2877 - j47.6105
4	Jebba-G	-0.289596 - j6.14081	-0.289596 - j6.14081	-27.3367 - j59.4155
5	Kainji	-0.295413 - j5.99661	-0.295413 - j5.99661	-25.326 - j56.2498
6	Mambilla	-0.401299 - j5.6904	-0.401299 - j5.6904	-22.9999 - j48.0256
7	Papalanto	-0.316098 - j4.62576	-0.316098 - j4.62576	-27.2532 - j52.5016

8	Sapele	-0.399808 - j5.75089	-0.399808 - j5.75089	-28.7473 - j50.3302
9	Shiroro	0.601244 - j11.9495	-0.601244 - j11.9495	-15.025 - j52.8714
10	Gwagwalada	-0.398682 - j5.78186	-0.398682 - j5.78186	-23.8332 - j47.0087
11	Lokoja	-0.398682 - j5.78186	-0.398682 - j5.78186	-23.8332 - j47.0087
12	Okpai	-0.39842 - j5.75232	-0.39842 - j5.75232	-23.1967 - j46.2208
13	Owerri	-0.398603 - j5.77241	-0.398603 - j5.77241	-23.6162 - j46.7129

Table 1 shows the comparative analysis of the eigenvalue result of the rotor angle, without governor, with governor, and with governor + power system stabilizer obtained from the eigenvalue graphs of figures 1, 2, and 3. It was observed that there were no changes when the systems ran without a controller and governor. It is not practicable to run a generator without a governor. The results showed that rotor angle (δ) was in a stable state for all 13 generators in the network with eigenvalues obtained having negative real parts with and without controllers; although a better system stability level was obtained with G + PSS compared to G because the real part of the obtained eigenvalues was much lower in value.

4. CONCLUSION In this work, we have quantitatively shown that the use of G + PSS produced better system stability level as compared with G only, because the real part of the obtained eigenvalues was much lower in value.

Acknowledgment: The authors wish to acknowledge support from other researchers for their valuable contributions.

Ethical Consideration: This work has no conflict whatsoever with any known ethical standards that require the seeking of permission and approval.

References

Afzal, H. Mokhlis, H. Azil Illias, N. Nadzirah Mansor, and H. Shareef. 2021. State-of-the-art review of power system resilience and assessment techniques. Int. Eng. Technol. 14(25): 6107-6121.

Mohammed, M., Roknuzzaman, K. M., Biswas, P. and Tanjimuddin, M. 2015. Stability Study of Power System. International Journal of Energy and Power Engineering, 4(2): 43-50.

Kawther Adam Eshag Mhmoud, Ahmed abdalla M. Imam, Ahmed Zakieldeen M. E. Elhassan H.H. 2021. Power System Dynamics and Stability. *Journal of Electrical and Electronics Engineering.* 16(2): 26-38.

D. Gohila, B.A. Carreras, J.M. Reynolds-Barredo, and P. Colet, O. Gomis-Bellmunt. 2023. Analysis of the blackout risk reduction when segmenting large power systems using lines with controllable power flow. *International Journal of Electrical Power & Energy Systems* 148(108947): 1–9.

Mohamed EL-Shimy 2018. POWER SYSTEM STABILITY: A technical report and a short course.

El Din H.M.Z. 1977. An Efficient Approach for Dynamic Stability Analysis of Power Systems including Load Effects. PhD Thesis. McMaster University, Hamilton, Ontario.

Chresta, A., Gonzalez-Longatt, and Francisco. 2021. Frequency Stability Issues and Research Opportunities in Converter Dominated Power System. *Energies.* 14(14): 4184.

Yousif Al Mashhadany, Ahmed K. Abbas, and Sameer Algburi. 2022. Study and Analysis of Power System Stability Based on FACT Controller System. *Indonesian Journal of Electrical Engineering and Informatics*. 10(2): 317–332.

Gross, G., Imperata, C.F. and Look, P.M. 1982. A Tool for the Comprehensive Analysis of Power System Dynamic Stability," IEEE Transactions on Power Apparatus and Systems, Vol. PAS-101, No. 1

undrica M. 2019. Speed control system of synchronous machine based on deterministic observers and feedback linearization method [PhD Thesis]. Zagreb.

J. K. Hwang and Y. Liu 2017. Identification of inter-area modes from ringdown data by curve-fitting in the frequency domain, *IEEE Transactions on Power Systems.* 32(4): 842–851.

. Suriya Devi, D. M., Shinshu, A., and Edward Wilson, S. 2021. Review of Power System Instability and Its Mitigation Techniques. *International Conference on Automation, Signal Processing, Instrumentation and Control*. Springer.

deMello, F. P. and Concordia, C. 1969. Concepts of Synchronous Machine Stability as Affected by Excitation Control. IEEE Trans. Power Apparatus and Systems, 92: 316-329.

Hall, M. C. 1975. Experience with 500 kV Subsynchronous Resonance and Resulting Turbine Generator Shaft Damage at a Mohave Generating Station. IEEE Summer Power Meeting, San Francisco, California.

S. S. Venkata, Mircea Eremia, and Lucian Toma. Background of Power System Stability. In book: Handbook of Electrical Power System Dynamics. pp 503–530

Ali Rahimzadeh, 2014–2015. POWER SYSTEM STABILIZER OPTIMIZATION IN LARGE ELECTRICAL NETWORKS.

G. Shahgholian. 2013. Review of the Power System Stabilizer: Application, Modeling, Analysis and Control Strategy. International Journal on Technical and Physical Problems of Engineering 5(3): pp 41- 52

Wang, J., Liang Z; Li Z; & Li, Y; Chuang Fu and Huang, L. 2017. Reactive power control strategy for low-power operation of HVDC transmission system. *Dianli Xitong Zidonghua/Automation of Electric Power Systems* 41(6): 154-158.

Falguni Bhavsar and Vijay H. Makwana. November. 2018. Impact of Stability in Power Systems and Techniques for Improvement. *Journal of Emerging Technologies and Innovative Research* 5(11): 609-614.

Neha Parsai and Alka Thakur. 2015. PV curve: Approach for Voltage Stability Analysis. *International Journal of Information Technology and Electrical Engineering* 4(2): 46–52.

Ochogwu Sunday Ope, Atuchukwu John and Obi Obinna Kingsley. 2019. Evaluation of the Power System Transient Stability of 330KV Nigeria Network. *ICONIC Research and Engineering Journals* 3(2): 433-438.

Engr. Aneel Kumar Akhani 2015 Engineering Articles Classification of Power System Stability.

K. R. Padiyar; and Anil M. Kulkarni. 2019. Analysis of Voltage Stability and Control in Dynamics and Control of Electric Transmission and Microgrids *IEEE*, pp. 283-309,

Yichen Zhou, Xiaohui Yang, Lingyu Tao, Li Yang. 2023. Transformer Fault Diagnosis Model Based on an Improved Gray Wolf Optimizer and Probabilistic Neural Network. Energies 16(7):3232.

Venkat Krishnan and James D. McCalley Submitted. 2012. Role of Induction Motors in Voltage Instability and Coordinated Reactive Power Planning. *InTech* 557pp.

A. A. Abdou, S. Kamel, M. Abdel-Akher, and F. Jurado. 2018. Voltage Stability Analysis of a Distribution Network in Egypt Including UPQC Device. *Twentieth International Middle East Power Systems Conference Cairo, Egypt.* pp. 1115-1120.

Moored, S., Wang, Y. and Chen, T. 2023. Novel collapse prediction index for voltage stability analysis and contingency ranking in power systems. Springer 8(7): 1- 27

Davidson, C., An, T., Hong, Z. 2023. HVDC Voltage Sourced Converters (VSC) and their Application for Power Transmission. High-Voltage DC Transmission Systems. CIGRE Green Books. Springer: pp 1-49

Alfredo Vaccaro and Antonio Pepiciello. 2022. Uncertain voltage stability analysis by affine arithmetic, Elsevier, pp. 123-133.

Hossain, J., Pota HR. 2014. Power System Voltage Stability and Models of Devices. In: Robust Control for Grid Voltage Stability: High Penetration of Renewable Energy. Power Systems. Singapore: Springe.,

Dr. Gitanjali Saha and Dr. Kabir Chakraborty. 2022. Application of Artificial Neural Networks in Power System Analysis. Book Rivers 169 pp.

Jožef Ritonja and Boštjan Polajžer. 2021. Analysis of the Local Mode Eigenvalues of Synchronous Generators in Modern Power Systems. Applied Sciences 32 pp.

Suraj Kumar and Priyajit Dash. 2016. Power Stability and Oscillation Damping Analysis of a Three Machine Nine Bus System. *International Journal of Innovative Research in Science, Engineering and Technology* 5(7): 12986–12996.

Sahar Azad, Reza Iravani, and Zeb Tate. (Apr 2015). Stability Enhancement of a DC Segmented AC Power System. IEEE Transactions on Power Delivery 30(2):737-745.

Peijie Li, Jinwang Hou, Yude Yang, and Xiaoqing Bai, 2023. Small signal stability constrained the optimal power flow model based on trajectory optimization. International Conference on Frontiers of Energy and Environment Engineering, Beihai, China 9(7): 489-499,

Hung Nguyen Dinh, Minh Y Nguyen, and Yong Tae Yoon. 2013. Novel Techniques for Real-Time Computing Critical Clearing Time (SIME-B and CCS-B. *Journal of Electrical Engineering and Technology* 8(2): 197-205.

Muralidhar Verma and Shriyansh Jain. 2017. Improving Power System Transient Stability by using Facts Devices. *International Journal for Technological Research in Engineering* 4(9): 1579-1582.

Fuhaid Basher, Mohamed I. El-sayed, and El-Saied Othman. 2016. Improving Dynamic Stability of Power Systems using AVR, a Power System Stabilizer. *International Journal of Electrical Engineering & Technology*. 10(2): 36–47.

Gibbard, M.J., Vowles, D.J., Pourbeik, P., 2015. Small-signal stability, control, and dynamic performance of power systems. University of Adelaide Press, 684 pp.

Ritonja, J.; Polajžer, B. Analysis of the Local Mode Eigenvalues of Synchronous Generators in Modern Power Systems. Applied Sciences: 32 pp.